J Mol Model (2013) 19:581–588
DOI 10.1007/s00894-012-1580-3

ORIGINAL PAPER

Insight on the interaction of polychlorobiphenyl with nucleic acid–base

Soraya Abtouche · Thibaut Very · Antonio Monari · Meziane Brahimi · Xavier Assfeld

Received: 13 July 2012 / Accepted: 21 August 2012 / Published online: 13 September 2012

Abstract The interaction between one polychlorobiphenyl (3,3′,4,4′,-tetrachlorobiphenyl, coded PCB77) and the four DNA nucleic acid–base is studied by means of quantum mechanics calculations in stacked conformations. It is shown that even if the intermolecular dispersion energy is the largest component of the total interaction energy, some other contributions play a non negligible role. In particular the electrostatic dipole-dipole interaction and the charge transfer from the nucleobase to the PCB are responsible for the relative orientation of the monomers in the complexes. In addition, the charge transfer tends to flatten the PCB, which could therefore intercalate more easily between DNA base pairs. From these seminal results, we predict that PCB could intercalate completely between two base pairs, preferably between Guanine:Cytosine pairs.

Keywords Charge transfer · Density functional theory · Dispersion interaction · DNA nucleobases · Electrostatic interaction · π stacking interaction · PolyChloroBiphenyl

Electronic supplementary material The online version of this article (doi:10.1007/s00894-012-1580-3) contains supplementary material, which is available to authorized users.

S. Abtouche · T. Very · A. Monari · X. Assfeld (✉)
Equipe de Chimie et Biochimie Théoriques, UMR 7565 CNRS
UL, Université de Lorraine,
BP 70239, 54506 Vandoeuvre-lès-Nancy, France
e-mail: Xavier.Assfeld@cbt.uhp-nancy.fr

S. Abtouche
Centre de Recherche Scientifique et Technique en Analyses Physico – Chimiques,
BP 248, Alger, RP 16004, Algerie

S. Abtouche · M. Brahimi
Laboratoire Physico Chimie Théorique et Chimie Informatique,
USTHB,
BP 32 EL ALIA 16111 BAB EZZOUAR,
Alger, Algerie

Introduction

Anthropogenic polychlorinated biphenyls (PCBs), that were widely used as industrial chemicals, accumulate in the environment as ubiquitous, persistent and highly lipophilic xenobiotics [1, 2]. These compounds tend to bioaccumulate and biomagnify, with a half-life of several months up to several years, because of their lipophilicity [3]. PCBs are known to be involved in immunosupression, neurotoxicity and endocrinal dysfunction [4]. They have been classified as probable human carcinogens by the International Agency for Research on Cancer (IARC) and have been implicated in several cancers such as hepatocellular carcinomas, trabecular carcinomas, adenocarcinomas and in diseases like cholangiomas, adenomas, and hepatomas [5]. Several mechanisms of action of PCBs have been proposed. PCBs without ortho substitution, for which a coplanar conformation is easily accessible, are shown to cause carcinogenicity through stimulation of cell proliferation [6]. They are metabolized by cytochrome P540 into arene oxide intermediates [7]. Upon metabolic activation, they are shown to bind to macromolecules such as DNA, RNA and protein [8]. A broad spectrum of biologic and toxic responses, of these classes of xenobiotics in animals, is mediated through the binding to a common cytosolic protein called the aryl hydrocarbon receptor (AhR) [9, 10]. The oxidative DNA damages induced by PCB and their implication in breast cancer has also been addressed [11].

3,3′,4,4′,5-pentachlorobiphenyl (PCB126) is the most toxic congener of all PCBs [12], and 3,3′,4,4′,5,5′-hexachlorobiphenyl (PCB169) is currently considered as toxic as 2,3,7,8-tetrachlorodibenzo-p-dioxin (TCDD) [13, 14]. In addition 3,3′,4,4′,-tetrachlorobiphenyl (PCB77), PCB126 [15] and PCB169 [16] have been shown to alter male reproductive development as TCDD does. PCB77 has been found in fish tissue [17], and can be transferred to human via the food. Sargent et al. [18] proposed that the clastogenic effects of PCB77 observed in human lymphocytes, may be

due to direct intercalation to DNA [19] and to a subsequent cascade of reactions [20]. The results of these previous experimental and theoretical studies lead to the conclusion that the interaction between polyhalogenated aromatics and biomolecules is mainly due to stacking [21].

In order to shed light on the main contributions (dispersion, electrostatic, charge transfer, …) of the interaction energy between PCBs and nucleic acid-bases, and prior to study the effects of PCBs on a double stranded DNA model, we decide to focus our attention on the interaction of PCB77 with the four DNA nucleic acid-bases (guanine (G), cytosine (C), adenine (A) and thymine (T)) by means of theoretical tools, studying complexes formed with one PCB77 molecule and one nucleic acid–base. These simple models will help to decompose the total interaction energy into insightful components and to determine the favored conformation PCBs could have while intercalated in DNA.

The next section contains the methodology and the computational details. The results are then discussed in the following section. The discussion is based on the analysis of the interaction energy at the equilibrium geometry and further detailed for some slightly distorted conformations in order to flesh out our knowledge of the potential energy hypersurface around the minimum.

Theory and computational details

In this present work, PCB77//DNA stacked complexes are optimized using three levels of theory, i.e., pure density functional theory (DFT) method within the local density approximation (LDA)—since it is computationally cheap and has been shown to produce acceptable results [22] certainly due to error compensation—, DFT-D techniques where empirical London dispersion energy terms are added to the usual functionals, and second-order Møller-Plesset theory (MP2), which correctly describes π stacking interactions. For LDA calculations, the Slater exchange functional was used in conjunction with the Vosko-Wilk-Nusair correlation functional (SVWN) [23] with the augmented polarized triple zeta quality 6-311++G** basis set. The Becke-Lee-Yang-Parr three parameters (B3LYP) exchange-correlation functional using the same basis set 6-311++G** was used for DFT-D computations using the empirical parameters developed by Grimme [24, 25]. The calculations have been performed using a local modified version of the quantum chemistry package Gaussian03 [26] that includes a generalized Grimme's dispersion correction. A general functional is modified with an empirical correction for long-range dispersion effects, described by a sum of damped interatomic potentials of the form C_6R^{-6} added to the usual DFT energy [25]. The total energy is given by:

$$E_{DFT-D} = E_{KS-DFT} + E_{disp}, \tag{1}$$

where $E_{KS\text{-}DFT}$ is the usual self-consistent Khon-Sham energy and E_{disp} is an empirical dispersion correction given by:

$$E_{disp} = -S_6 \sum_{i=1}^{N_{at}-1} \sum_{j=i+1}^{N_{at}} \frac{C_6^{ij}}{R_{ij}^6} f_{damp}(R_{ij}). \tag{2}$$

Here, N_{at} is the number of atoms in the system, C_6^{ij} denotes the dipole-dipole dispersion coefficient for atom pair ij, S_6 is a global scaling factor that only depends on the functional used, and R_{ij} is the interatomic distance. In order to avoid near–singularities for small R, a damping function f_{damp} must be used,

$$f_{damp}(R_{ij}) = \frac{1}{\left(1 + \exp\left(-\alpha\left(\frac{R_{ij}}{R_0 - 1}\right)\right)\right)}, \tag{3}$$

where R_0 is the sum of atomic van der Waals radii and α is the parameter determining the steepness of the damping function. The value of the atomic C_6 coefficients, R_0, α and S_6 parameters as well as the combination rule for the composite C_6^{ij} coefficients were taken from the work of Grimme [24, 25].

Due to the inherent more important computational cost for MP2 calculations, the medium quality 6-31G* basis set was used, as it was shown to give a good compromise between accuracy and computational cost [27–29].

Geometries of the complexes of PCB77 with DNA nucleobases were fully optimized at the three levels of theory. The nature of the critical points was confirmed by inspection of the Hessian matrix. The absence of negative eigenvalues confirming that the obtained geometries are real minima on the potential energy hypersurface.

The interaction energy $\Delta E^{A//B}$ of a stacked complex A//B (// denotes stacking) is defined as the electronic energy difference between the energy of the complex ($E^{A//B}$) and the energies of the isolated molecules (E^A, E^B)

$$E_{int} = \Delta E^{A//B} = E^{A//B} - \left(E^A + E^B\right). \tag{4}$$

Results and discussion

Interaction energies at equilibrium geometry

The interaction energies, obtained at the SVWN/6-311++G**, MP2/6-31G* and B3LYP-D/6-311++G** levels of theory, of the optimized complexes are reported in Table 1. The corresponding geometries are drawn in Fig. 1.

Table 1 Interaction energies between PCB77 and DNA nucleobases (ΔE, kcal mol^{-1}) at the three levels of theory

	$\Delta E^{PCB77//G}$	$\Delta E^{PCB77//A}$	$\Delta E^{PCB77//C}$	$\Delta E^{PCB77//T}$
SVWN/6-311++G**	−20.63	−16.19	−18.35	−17.16
MP2/6-31G*	−18.02	−14.93	−15.17	−13.92
B3LYP-D/6-311++G**	−18.48	−14.45	−15.67	−15.16

Several features can be observed from the values reported in Table 1. One can note that, although the values are different, the three methods predict the PCB77//G complex to be the most stable, and the PCB77//C complex to be the second more stable. The two DFT based methods show larger interaction energy for the PCB77//T complex compare to PCB77//A, whereas MP2 gives the reverse order of stability. Anyway, the energy differences being about 1 kcal mol^{-1}, one cannot draw definitive conclusions with these levels of theory. It is remarkable to note that the three levels of theory are in a very good mutual agreement with differences in the interaction energy of about 2 kcal mol^{-1} at maximum. DFT-D and MP2 methods give very similar results, when LDA gives stronger interactions by 2 kcal mol^{-1}.

The optimized geometries, obtained with the three methods are very similar and the cartesian coordinates are given in the supplementary material. The geometry of the constituent molecules (i.e., PCB77 or the nucleobase) in the complexes is very similar to the geometry of the isolated molecules. This could have been anticipated for weakly interacting molecules. One can note that PCB77 is not planar in the complexes (neither in the isolated molecule), which means that the interaction energy with the nucleic base is not large enough to overcome the rotation barrier around the central C–C bond of the biphenyl moiety, due to the steric hindrance of the atoms in ortho positions. As a consequence the nucleobase interacts mainly with one phenyl ring of PCB77.

Table 2 Variation of the interaction energy (in kcal mol^{-1}) for a vertical separation of 0.4 Å longer than the equilibrium value, at the three levels of theory SVWN/6-311++G**, B3LYP-D/6-311++G** and MP2/6-31G*

	PCB77//G	PCB77//A	PCB77//C	PCB77//T
SVWN/6-311++G**	0.34	0.81	0.60	1.09
MP2/6-31G*	0.07	0.61	0.19	0.41
B3LYP-D/6-311++G**	0.19	0.31	0.28	0.89

Our results confirm [27, 30] that LDA calculations can give quite satisfying stacking energy and geometries, at least for the equilibrium geometry. In order to better understand the possible interactions with DNA, we decided to analyze other regions of the potential energy hypersurface for some selected degrees of freedom that can be relevant for intercalation. The results are gathered in the next subsection.

Vertical separation

The distance between the molecules is called the vertical separation (VS). It is defined as the distance between the centers of mass of both molecules. Starting from the equilibrium geometry, the intermolecular distance (VS) was stretched by 0.4 Å, and all other geometrical parameters optimized. The energy variations from the equilibrium geometry to the stretched one are collected in Table 2.

One can note that, more or less, LDA gives values about twice as large as those obtained with DFT-D, which are almost double than those obtained with MP2. This discrepancy between DFT and perturbation theory can arise because of the medium quality basis set used in MP2 calculations. Since diffuse and polarization functions are missing, the intermolecular interaction is less well described at long distance. Although

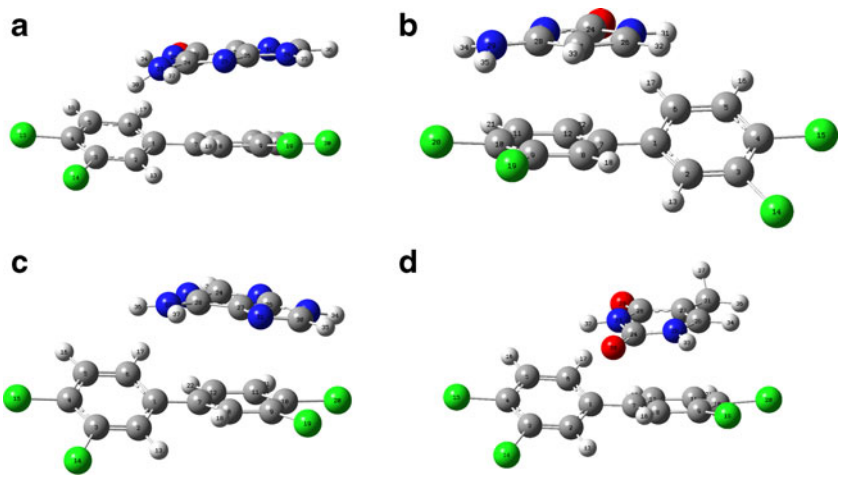

Fig. 1 Optimized geometries, obtained at the B3LYP-D/6-311++G** level of theory. (**a**) PCB77//G, (**b**) PCB77//C, (**c**) PCB77//A, (**d**) PCB77//T

Table 3 Variation of the interaction energy (in kcal mol^{-1}) for a vertical separation of 0.2 Å less than the equilibrium value, at the SVWN/6-311++G** level of theory

	PCB77//G	PCB77//A	PCB77//C	PCB77//T
SVWN/6-311++G**	0.25	1.29	1.11	0.87

the absolute values are different, the trends are similar for the two DFT levels of theory. One can define the following order: G>C>A>T, the complex containing G nucleic acid–base being the easiest one to stretch along the vertical separation. This point has to be compared with the results found in the previous subsection. Albeit the complexes formed with PCB77 and either Thymine or Adenine are less energetically favorable (see Table 1), they are more firmly bound (in the sense that the wells along the VS coordinate are steeper for these two complexes). This means that for these two complexes the short range attractive components of the interaction energy varies more steeply than those of the complexes composed of PCB77 and Cytosine or Guanine, suggesting that more than one interaction factor can indeed be present. This point will be discussed in more detail in the following subsection.

When PCB77 intercalates between DNA base pairs, the intermolecular distance (during the intercalation process) can be shorter than the equilibrium distance presented in the previous subsection. Hence, the squeezing of the vertical separation can provide some insights on the ease of PCB77 to intercalate in DNA. The VS was shortened by 0.2 Å compared to the equilibrium value, since for a squeezing of 0.4 Å one encounters the repulsion wall that is almost universal. Only SVWN results are presented and are gathered in Table 3.

One can note that for Guanine, the repulsion is the smallest compared to the other nucleic acid bases. This shows that at this very short range an attractive interaction takes place for this complex, that partially compensates the repulsion. These results suggest a possible selectivity of PCB77 upon interaction with DNA, Guanine sites being the most plausible candidates for intercalation.

Relative orientation

In this subsection, the relative orientation of PCB77 and the nucleic acid bases is considered. Relaxed scans were performed along the dihedral angle Φ defining the relative orientation of the two molecules using steps of 30° and starting from the equilibrium geometry. The dipole-dipole interaction between the two molecules forming the complex is examined.

In Fig. 2, the interaction energy together with the total dipole moment of the complex are plotted with respect to the dihedral angle Φ.

As can be seen, the calculated total interaction energy (E_{int}) strongly depends on the relative orientation of the molecules in the complex. One can note that the lower energy conformation is in a region where the total dipole moment is low, showing that the dipoles of the PCB and of the nucleic acid–base adopt an anti-parallel orientation. This proves that the dipole-dipole interaction component of the

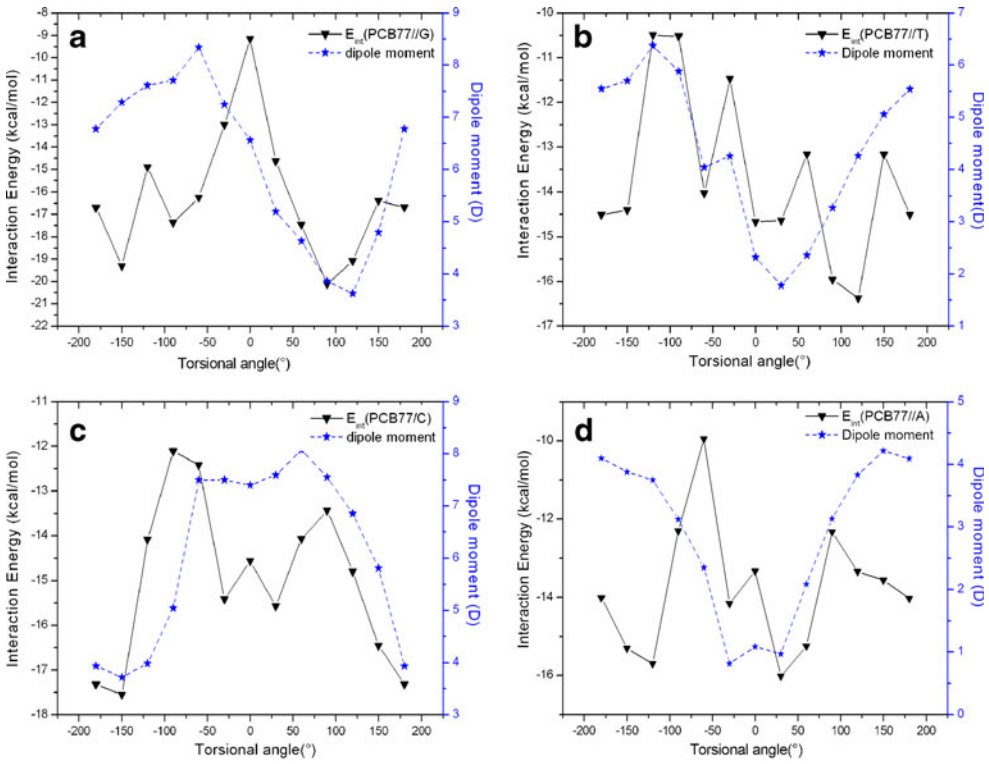

Fig. 2 Interaction energy in kcal mol^{-1} (solid black line) and dipole moment in Debye (dotted blue line) with respect to the dihedral angle between PCB77 and DNA nucleobases, at the SVWN/6-311++G** level of theory. (**a**) PCB77/G complex, (**b**) PCB77//T complex, (**c**) PCB77//C complex, (**d**) PCB77//A complex

Table 4 Intermolecular dispersion energy (in kcal mol^{-1}) computed at the B3LYP-D/6-311++G** level of theory for the four complexes

	PCB77//G	PCB77//A	PCB77//C	PCB77//T
ΔE_{disp}	−19.15	−16.96	−15.40	−15.17

Table 6 The transferred charge from nucleobases to PCB77 for each complex

	PCB77//G	PCB77//C	PCB77//A	PCB77//T
Q (e)	0.227	0.125	0.016	0.004

total interaction energy is responsible for the relative orientation of the two molecules in the complex. However, if the value of Φ corresponding to the minimum of the interaction energy is close to the one for the smallest dipole moment, the two values are not exactly coincident. This fact shows that some other orientation dependent contributions, like charge transfer, cannot be neglected.

Up to now, we have discussed the total interaction energy for different geometries in order to understand the relative orientation of the molecules in the complexes and total binding interaction. We now turn to a decomposition of the total interaction energy into insightful main components.

Dispersion energy

From DFT-D calculations, it is straightforward to extract the intermolecular dispersion energy for the equilibrium structure (see Eq. 1). Results are given in Table 4. One can see that, compared to the values given in Table 1 for the DFT-D level of theory, the intermolecular dispersion energy is of the same magnitude as the total interaction energy. It is even higher for Guanine and Adenine nucleobases. Although, this term is certainly the leading one, it is not the only one. In particular, as shown above, dipole-dipole interactions are certainly responsible for the relative orientation of the molecules in the complex, and charge transfer can also play a non trivial role. These two components are further discussed below.

Dipole-dipole interaction

To clarify the slight offset between the optimized geometry and the geometry corresponding to the lowest total dipole moment, we decided to have a deeper look into the dipole-dipole interaction. The geometrical distortion of PCB77 and the nucleobases upon complexation is considered. The total dipole moment of the complex is compared to the one obtained by the simple vector addition of the individual dipole moments of PCB77 and the nucleobases at the complex geometry. All results are gathered in Table 5.

It is noteworthy that, for each fragment, the dipole moment is higher in the geometry of the complex than for the geometry of the monomer. This shows that the slight geometry distortion produces higher dipole moments to induce a higher dipole-dipole attractive interaction. This is in perfect agreement with the fact that the total dipole moment is lower than the one computed with the additive model, due to inductive interactions. This conclusion was previously reported for π–π interactions between other biomolecules [31, 32].

Charge transfer

The charge transfers were determined using the Mulliken population analysis [33] (Table 6) at the SVWN/6-311++G** level of theory. Although Mulliken's partitioning is a crude model it can be useful to represent trends and give qualitative insights for a comparative study. The charge transfer between the molecules within the complex is essentially one directional (occurring from DNA nucleobases to PCB77) and predominantly of π-π^* type. If the charge transfer is practically negligible for A and T nucleobases, it is several order of magnitude larger for C and G. The peculiar role of G is once more evidenced. The amount of charge transfer (Q) increases going from Thymine, to Adenine, to Cytosine, and finally to Guanine. This order is similar to the one found for the total interaction energy, and could explain the low energy raise when the PCB77//G complex is squeezed (the shorter the intermolecular distance, the higher the charge transfer).

Table 5 Dipole moment (in debye, D) of the molecules PCB77 and the four DNA nucleobases, in their optimized geometries (μ^m) and in the geometry of the complex (μ^c). Total dipole moment of the complex as computed with G03 (μ^T) and by the vector addition of the dipole moment of the constituting molecules (μ^{add}), at the SVWN/6-311++G** level of theory

	PCB77	A	T	G	C
μ^m	2.23	2.48	4.42	6.91	6.70
μ^c	2.47	2.67	4.55	6.96	6.76
		PCB77//A	PCB77//T	PCB77//G	PCB77//C
μ^T		1.32	3.89	3.94	3.75
μ^{add}		1.35	4.12	4.44	4.41

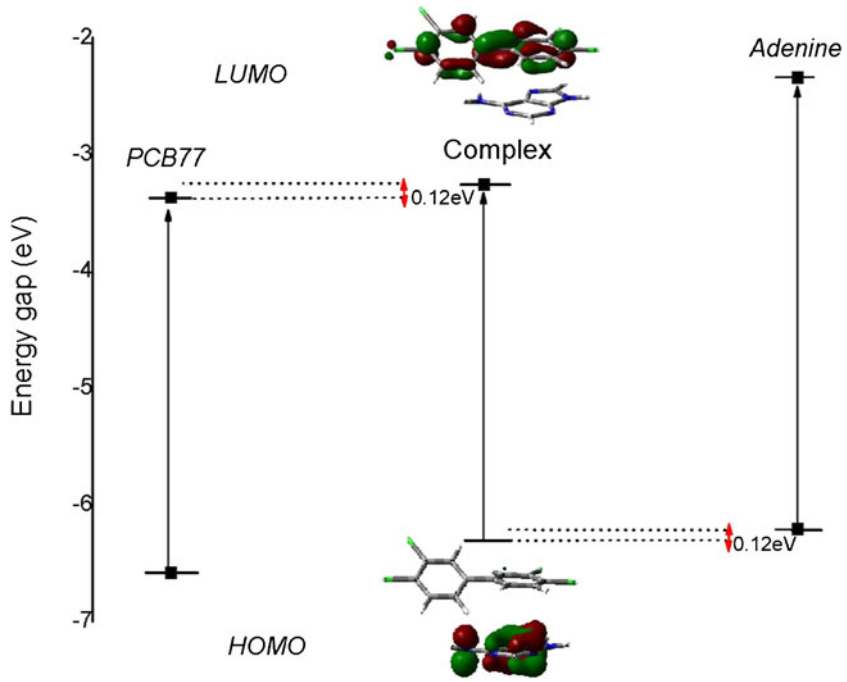

Fig. 3 Calculated LUMO-HOMO energy levels of the complex, compared to the respective levels of isolated PCB77 (*left*) and Adenine (*right*) molecules

A molecule with a planar geometry is more inclined to intercalate in DNA than a globular molecule, and can thus be more toxic. The toxicity of PCB77 can be related to the charge transfer, since the latter induces a more planar geometry of PCB77—the dihedral angle between the two phenyl rings is close to 31–32° for all complexes, compared to the value close to 33° for the isolated molecule. This is consistent with the optimized geometry of PCB77 anion, at the same level of theory, where the dihedral angle between the two phenyl rings is zero.

The charge transfer and the increased planarity can be interpreted by means of the frontier molecular orbitals (HOMO and LUMO). One has to note that the LUMO of the isolated PCB77 presents a bonding interaction between the two carbon atoms bridging the phenyl groups (see Fig. 3). Hence, upon partial electron capture, PCB77 tends to flatten. Figure 3 presents the interaction diagram between the HOMO of adenine (given as an example) and the LUMO of PCB77, to produce the frontier orbitals of the complex. The latter are indistinguishable to the former. One can see that the charge transfer occurs from the DNA nucleobase (acting as a nucleophile) to PCB77 (acting as an electrophile).

Prediction of intercalation in DNA

Although the intercalation process is much more complicated, involving for instance DNA deformation, possible hydrogen bond rupture or weakening between nucleobases, loss of π stacking between adjacent nucleobases, desolvatation, … than the simple bimolecular interaction considered here, from the results presented in this work, we can try to foresee the preferred intercalation sites. A PCB77 molecule can be intercalated in DNA in two main ways: either by a partial intercalation where one aromatic ring fits between two nucleobases belonging to adjacent base pairs (the central C−C bond of PCB77 is more or less perpendicular to the H-bond network linking two nucleobases), or by a complete intercalation where the two aromatic rings slide between two base pairs (the central C−C bond of PCB77 is approximately parallel to the H-bond network linking two nucleobases). By inspection of the optimized geometries, we can see that PCB77 adopts an orientation favorable for the intercalation of the two aromatic rings for Guanine, Cytosine and Thymine. For Adenine, both intercalations are possible. Anyway, due to the fact that the energy variation upon rotation is weak—close to 5 $kcal\,mol^{-1}$ (see Fig. 2), and smaller than the interaction energy (Table 1), we can conclude that the complete intercalation is certainly the most favorable one. In addition, from the interaction energies given in Table 1, we can predict that PCB77 will intercalate preferentially between two G:C base pairs (either G:C/G:C or G:C/C:G). The second preferred type of site is G:C/T:A (or G:C/A:T). The less favorable site is composed of two T:A base pairs. These predictions are in good agreement with our preliminary results where PCB77 interacts with a double stranded DNA, studied by means of hybrid quantum mechanics/molecular mechanics (QM/MM) calculations.

Conclusions

The interaction between one polychlorobiphenyl (PCB77) and the four DNA nucleic acid bases has been studied by means of quantum chemistry methods. Due to error compensation, LDA level gives accurate qualitative predictions in good agreement

with DFT-D and MP2 levels of theory. Even if the dispersion energy is the largest component of the total interaction energy, other contributions cannot be neglected. In particular, the complexes adopt a conformation where the dipole moments of the constituting molecules are anti-parallel. These orientations are also responsible for the correct overlap between the frontier orbitals, giving an intermolecular charge transfer. In consequence, PCB77 adopts a more planar geometry which will ease the intercalation process. From geometrical and energetic considerations, we predict that PCB77 will intercalate completely between two G:C base pairs preferentially.

In a forthcoming work the intercalation of PCB77 in a double stranded DNA will be studied by means of hybrid QM/MM calculations.

Acknowledgments SA is very thankful to the Algerian government for a bursary. AM and XA thank the Agence National de la Recherche for funding ANR-09-BLAN-0191-01 PhotoBioMet.

References

1. Jimenez B, Wright C, Kelly M, Startin JR (1996) Levels of PCDDs, PCDFs and non-ortho PCBs in dietary supplement fish oil obtained in spain. Chemosphere 32:461–467
2. Kurokowa Y, Matsueda T, Nakamura M, Takada S, Fukamachi K (1996) Characterization of non-ortho coplanar PCBs, polychlorinated dibenzo-p-dioxines and dibenzofurans in the atmosphere. Chemosphere 32:491–500
3. Morgan DP, Roan CC (1971) Absorption, storage, and metabolic conversion of ingested DDT and DDT metabolites in man. Arch Environ Health 22:301–308
4. Kimbrough RD (1995) Polychlorinated biphenyls (PCBs) and human health: an update. Crit Rev Toxicol 25:133–163
5. Faroon OM, Keith S, Jones D, De Rosa C (2001) Carcinogenic effects of polychlorobiphenyls. Toxicol Ind Health 17:41–62
6. Safe SH (1994) Polychlorinated biphenyls (PCBs): environnemental impact, biochemical and toxic responses, and implications for risk assessment. Crit Rev Toxicol 24:87–149
7. Preston BD, Miller JA, Miller EC (1984) Reactions of 2,2′,5,5′-tetrachlorobiphenyl 3,4-oxide with methionine, cysteine and glutathione in relation to the formation of methylthio-metabolites of 2,2′,5,5′-tetrachlorobiphenyl in the rat and mouse. Chem Biol Interact 50:289–312
8. Narbonne JF, Daubeze M (1980) In vitro binding hexachlorobiphenyl to DNA and proteins. Toxicology 16:173–175
9. Poland A, Glover E, Kende AS (1976) Stereospecific high binding affinity of 2,3,7,8-teratchlorodibenzo-p-dioxin by cytosols. Evidence that the binding species is a receptor for induction of aryl hydrocarbon hydroxylase. J Biol Chem 251:4936–4946
10. Cheney BV, Tolly T (1979) Electronic factor affecting receptor binding of binding of dibenzo-p-dioxins and dibenzofurans. Int J Quant Chem 16:87–110
11. Parthasarathi R, Padmanabhan J, Sbramanian V, Maiti B, Chattaraj PK (2003) J Phys Chem A 107:10346–10352
12. Yoshimura H, Yoshihara S, Ozawa N, Miki M (1979) Possible correlation between induction modes of hepatic enzymes by PCBs and their toxicity in rats. Ann NY Acad Sci 320:179–192
13. Jimenez B, Hernandez LM, Eljarrat E, Rivera J, Gonzalez MJ (1996) Level of PCDDs, PCDFs, and non-ortho PCBs in serum samples of non-exposed individuals living in Madrid (Spain). Chemosphere 33:2403–2410
14. Tanabe S, Kannan N, Wakimoto T, Tatsukawa R (1987) Method for the determination of three toxic nonortho chlorine substituted coplanar PCBs in environmental samples at part-per-trillion levels. Int J Environ Anal Chem 29:199–213
15. Faqi AS, Dalsenter PR, Merker HJ, Chahoud I (1998) Effects on developmental landmarks and reproductive capability of 3,3′,4,4′-tetrachlorobiphenyl and 3,3′,4,4′-pentachlorobiphenyl in offspring of rats exposed during pregnancy. Hum Exp Toxicol 17:365–372
16. Gray LE Jr, Wolf C, Mann P, Price M, Cooper RL, Ostby J (1999) Adminstration of potentially antiangenic pesticides and toxic substances (dibutyl- and dielthyl hexyl phtalate, PCB169, and ethane dimethane sulfonate) during sexuel differentiation produces divers profiles of reproductive malformations in the male rate. Toxicol Ind Health 15:94–118
17. Hong C, Bush B, Xiao J (1992) Coplanar PCBs in fish and mussels from marine and estuarine waters of New York states. Ecotoxicol Environ Safety 23:118–131
18. Sargent S, Roloff B, Meisner L (1989) In vitro chromosome damage due to PCB interactions. Mutat Res 224:79–88
19. Wasson JS, Huff JE, Loprieno N (1977) A review of the genetic toxicology of chlorinated dibenzo-p-dioxins. Mutat Res 47:141–160
20. Poland A, Glover E (1980) 2,3,7,8-tetrachlorodibenzo-p-dioxin: segregation of toxicity with the Ah locus. Mol Pharmacol 17:86–94
21. Safe S (1986) Comparative toxicology and mechanism of action of polychlorinated dibenzofurans. Annu Rev Pharmacol Toxicol 26:371–399
22. Swart M, Wijst TV, Guerra CF, Bickelhaupt FM (2007) π-π stacking tackled with density functional theory. J Mol Model 13:1245–1257
23. Vosko SH, Wilk L, Nusair M (1980) Accurate spin-dependent electron liquid correlation energies for local spin density calculations: A critical analysis. Can J Phys 58:1200–1211
24. Zimmerli U, Parrinello M, Koumoustsakos P (2004) Dispersion corrections to density functionals for water aromatic interactions. J Chem Phys 120:2693–2699
25. Grimme S (2004) Accurate description of van der Waals complexes by density functional theory including empirical corrections. J Comput Chem 25:1463–1473
26. Frisch MJ, Trucks GW, Schlegel HB, Scuseria GE, Robb MA, Cheeseman JR, Montgomery JA Jr, Vreven T, Kudin KN, Burant JC, Millam JM, Iyengar SS, Tomasi J, Barone V, Mennucci B, Cossi M, Scalmani G, Rega N, Petersson GA, Nakatsuji H, Hada M, Ehara M, Toyota K, Fukuda R, Hasegawa J, Ishida M, Nakajima T, Honda Y, Kitao O, Nakai H, Klene M, Li X, Knox JE, Hratchian HP, Cross JB, Bakken V, Adamo C, Jaramillo J, Gomperts R, Stratmann RE, Yazyev O, Austin AJ, Cammi R, Pomelli C, Ochterski JW, Ayala PY, Morokuma K, Voth GA, Salvador P, Dannenberg JJ, Zakrzewski VG, Dapprich S, Daniels AD, Strain MC, Farkas O, Malick DK, Rabuck AD, Raghavachari K, Foresman JB, Ortiz JV, Cui Q, Baboul AG, Clifford S, Cioslowski J, Stefanov BB, Liu G, Liashenko A, Piskorz P, Komaromi I, Martin RL, Fox DJ, Keith T, Al-Laham MA, Peng CY, Nanayakkara A, Challacombe M, Gill PMW, Johnson B, Chen W, Wong MW, Gonzalez C, Pople JA (2004) Gaussian03, revision B.05. Gaussian, Inc, Wallingford
27. Sponer J, Leszczynski J, Hobza P (1996) Nature of nucleic acid−base stacking: nonempirical ab initio and empirical potential characterization of 10 stacked base dimers. Comparison of stacked and H-bonded base pairs. J Phys Chem 100:5590–5596
28. Hobza P, Sponer J (1999) Structure, energetics, and dynamics of the nucleic acid base pairs: nonempirical Ab initio calculations. Chem Rev 99:3247–3276
29. Sponer J, Florian J, Ng HL, Sponer JE, Spackova N (2000) Local conformational variations observed in B-DNA crystals do not

improve base stacking: computational analysis of base stacking in a d(CATGGGCCCATG)$_2$ B↔A intermediate crystal structure. Nucleic Acids Res 28:4893–4902
30. Swart M, Ehlers AW, Lammertsma K (2004) Performance of the OPBE exchange-correlation functional. Mol Phys 102:2467–2474
31. Cassandra DM, Wetmore C, Wetmore SD (2009) Noncovalent interactions involving histidine: the effect of charge on π−π stacking and T-shaped interactions with the DNA nucleobases. J Phys Chem B 113:16046–16058
32. Rutledge LR, Wheaton CA, Wetmore SD (2007) A computational characterization of the hydrogen-bonding and stacking interactions of hypoxanthine. Phys Chem Chem Phys 9:497–509
33. Mulliken RS (1955) Electronic population analysis on LCAO MO molecular wave functions I. J Chem Phys 23:1833–1840